# Peculiarities of Ruby Synthesized from $Al_2O_3$–$Cr_2O_3$ Powder Mixture by Selective Laser Sintering

M. Vlasova[a*], M. Kakazey[a], P. A. Márquez Aguilar[a], R. Guardian Tapia[a], E .A. Juarez Arellano[a], V. Stetsenko[b], A. Ragulya[b], A. Bykov[b], I. Timofeeva[b]

[a]*Research Center in Engineering and Applied Sciences of the Autonomous University of the State of Morelos (CIICAp-UAEMor), Av. Universidad, 1001, Cuernavaca, Mexico.*
[b]*Institute for Problems of Materials Science, National Academy of Sciences of Ukraine, 3, Krzhyzhanovsky St., Kiev, 252680, Ukraine*

**Abstract:** The synthesis of ruby from an $Al_2O_3$–$Cr_2O_3$ mixture compacted in pellets of different density by layer-by-layer selective laser sintering (SLS) has been investigated depending on the irradiation power and the traverse speed of a laser beam. It has been established that a formed track consists of crystallites textured: vertical texturing is inherent to volume layers and horizontal texturing is proper to surface layer. The morphology of the surface of the track is determined by the irradiation conditions.

DOI:10.2961/jlmn.2011.02.0001
**Key words:** $Al_2O_3$–$Cr_2O_3$ compact, laser treatment, ruby track.

## 1. Introduction

It is known that corundum ($\alpha$-$Al_2O_3$) has found an extensive use in different fields of engineering [1]. In recent years, the method of synthesis of corundum ceramics by selective laser sintering has been developed [2–7]. Among corundum-based ceramics, ruby, which is a solid solution of chromium ions in the solid structure of covalent $Al_2O_3$, is the most extensively used material. Ruby single crystals are used as working elements of lasers. A single crystal laser medium is usually limited by its size and the amount of optically active elements [8]. For the solution of these problems, it is interesting to use polycrystalline corundum with chromium oxide additives treated by the layer-by-layer SLS technology. It is assumed that, in the framework of SLS, it is possible to combine chromium diffusion into the aluminum oxide lattice with the sintering, melting, and crystallization of the disperse system.

Preliminary investigations of the synthesis of ruby by layer-by-layer SLS of an $Al_2O_3$–$Cr_2O_3$ powder mixture [9] shows that the obtainment of a homogeneous ruby material within the limits of the given technology is a difficult problem and requires the careful selection of parameters such as the irradiation power, the laser beam traverse speed, the height and the number of prepared layers.

The purpose of the present work is to investigate further the features of the formation of ruby layers on a surface of loose and dense $Al_2O_3$–$Cr_2O_3$ compacts.

--*Corresponding author: vlasovamarina@inbox.ru;

## 2. Materials and Methods of Preparation and Investigation

In the work, commercially available $Al_2O_3$ and $Cr_2O_3$ (Reasol, ReactivoAnalitico, Mexico City) powders were used. The particle sizes of the $Al_2O_3$ and $Cr_2O_3$ powders were 40 nm and 1.8 μm, respectively. On the base of these powders, a 97 wt. % $Al_2O_3$ + 3 wt. % $Cr_2O_3$ mixture was prepared, from which two types of pellets were pressed. Pellets of the first type with a diameter of 30 mm and a height of 3 mm were compacted under an axial pressure of 5 MPa, and pellets of the second type with a diameter of 4 mm and a height of 4 mm were pressed under an isostatical pressure of 5 GPa.

Targets were irradiated with a continuous-action laser with a wave length $\lambda$ = 1064 μm (LTN-103 facility, Russia). For the laser synthesis, the following values of the irradiation power (P) were chosen: 60, 70, 160, and 190 W. The diameter of the laser spot was 0.2 mm. A laser beam was traversed over the surfaces of pellets at traverse speeds of a coordinate table (v) of 0.075, 0.15, 0.3, 0.7, and 1.25 mm/s. The system of vertical movement of a sample without changing the size of the laser spot enabled us to carry out additional operations on the surface of pellets.

Using the laser facility, one-pass and four-pass (along the same path) treatments of the surface of a pellet were performed. In the former case, a channel formed on the surface. In the latter case, after the first pass of the laser beam, a specimen was lowered to a height of 280 μm. The formed track was filled with the powder mixture, which was then pressed and leveled. The height of the backfill (h) was

280 μm. The filled channel was irradiated again. The backfilling procedure was performed thrice. As a result, a four-layer track was formed.

An electron microscopy study was performed with a Superprobe-733 scanning electron microscope (JEOL, Japan) and a SEM/FIB NOVA 200 system (Bruker, Gemany). An X-ray diffraction (XRD) analysis of the specimens was carried out using a Siemens D-500 diffractometer (Munich, Germany) in Cu $K_\alpha$ radiation. EPR investigations were performed with an X-band microwave spectrometer at room temperature (SE/X 2547-Radiopan, Poznan, Poland).

## 3. Experimental Results

After irradiation, on the surfaces of specimens, red tracks formed.

### 3.1. X-ray and EPR data

According to the XRD data, the main phase of the powder compacts is $Al_2O_3$ (corundum), which has a hexagonal lattice with constants $a$ = 0.476 nm and $c$ = 1.299 nm. For tracks formed by layer-by-layer SLS, the interplanar spacing ($d$) initially diminishes and then rises as the number of layers and irradiation intensity increase (see **Table I**). The obtained results can be explained by the fact that, at first, $Cr_2O_3$ gradually dissolves in $Al_2O_3$, and then a part of chromium leaves earlier formed aluminum–chromium oxide.

**Table I**. Change of $d_{100}$ in aluminum–chromium oxide after laser treatment in different conditions

| Laser treatment type | $d_{100}$, nm | Lattice type |
|---|---|---|
| Initial compacted mixture | 0.2084 | corundum |
| One-run treatment, P = 120 W, v = 1.25 mm/s | 0.2069 | aluminum chromium oxide (ruby) |
| 2 layers of the backfill, P = 120 W, v = 0.64 mm/s | 0.2075 | aluminum chromium oxide (ruby) |
| 4 layers of the backfill, P = 120 W, v = 1.25 mm/s | 0.2076 | aluminum chromium oxide (ruby) |
| 4 layers of the backfill, P = 160 W, v = 1.25 mm/s | 0.2078 | aluminum chromium oxide (ruby) |

In the initial mixture, only a weak broad EPR signal, which is due to the defective states of the α–$Cr_2O_3$ phase, is observed at g ~ 1.9. For red tracks, EPR lines are registered at $g_I \approx 1.22$, $g_{II} \approx 1.47$, $g_{III} \approx 3.38$, and $g_{IV} \approx 22$ (**Fig. 1**). This spectrum is typical of polycrystalline ruby [10, 11]. Thus, in the irradiation zone of pellets, ruby is synthesized.

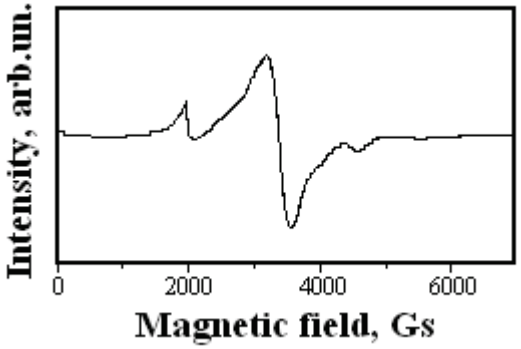


**Fig.1.** EPR spectrum of a 97 wt. % $Al_2O_3$–3 wt. % $Cr_2O_3$ laser treated sample.

### 3.2. Electron microscopy data of irradiated axially pressed pellets

The surface of a track after a single pass of the laser beam is shown in **Fig. 2 a**. On the surface, one can see arcs. Theirs formation is a result of melting → cooling of corundum during transverse of the laser beam. On the lateral walls of the channel, strips formed as a result of dissociation of $Al_2O_3$ (**Fig. 2 b**) are seen.

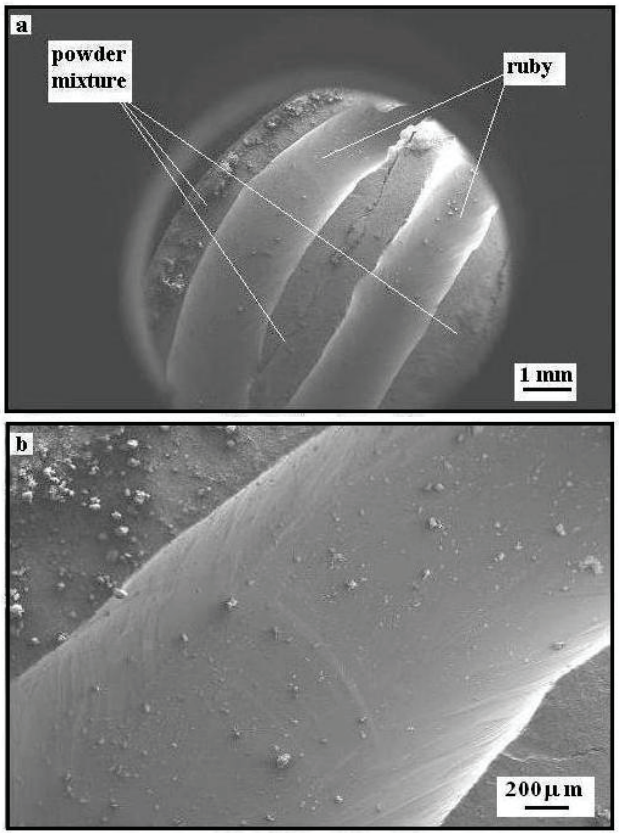

**Fig. 2.** Micrographs of channels formed in one-pass laser treatment of a compact at P = 160 W and v = 1.25 mm/s.

In a cross-section of the channel, zones of different colors are clearly seen (**Fig. 3**). The darkest (red) zone is a zone of melting-recrystallization of alumina. Under the red layer, lighter (pink) layer of sintered corundum with $Cr^{3+}$ ions lies. The lowest grey-greenish layer is the "initial"$Al_2O_3$–$Cr_2O_3$ mixture. Zones of recrystallization and sintering have a conical shape, which is due to the "defocusing" of the laser beam.

The defocusing results in a decrease in the power of the laser beam in a peripheral zone, and, consequently, in a decrease in the heating temperature. In **Fig. 4,** the growth of corundum crystallites from the bottom part of the track to its surface is shown.

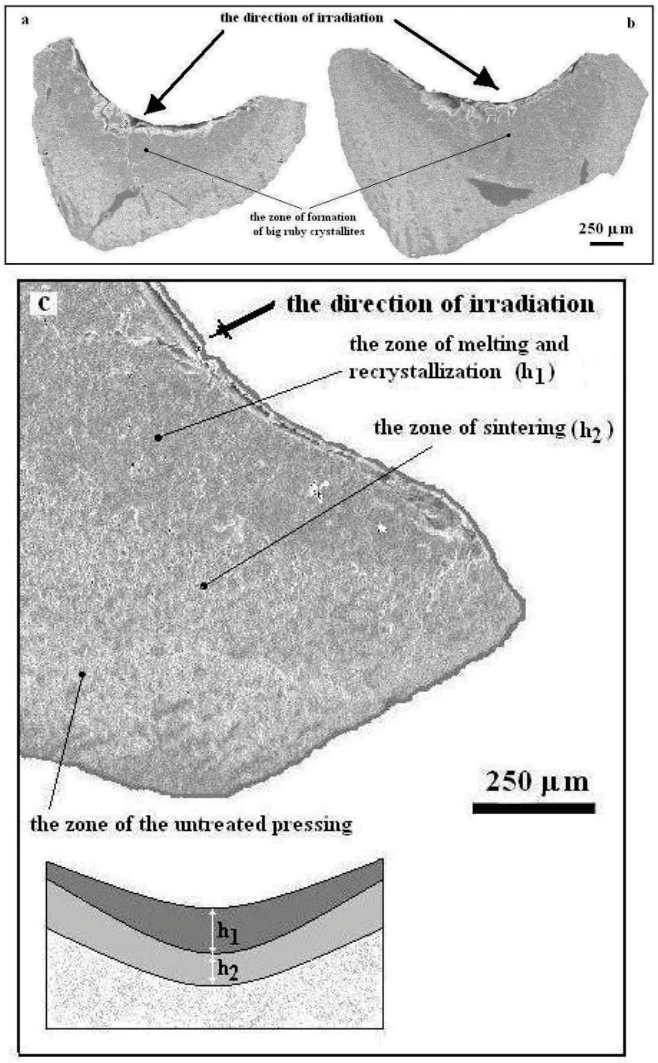


**Fig. 3.** Micrographs of channels formed in one-pass laser treatment of a compact at P = 60 W (a) and 70 W (b) and v = 0.3 mm/s; (c) is a fragment of an irradiated pellet with designations of formed zones.

The depth of the channel depends on irradiation parameters, namely, the irradiation power and the traverse speed of the laser beam. Thus, with increase in the irradiation power (P), the thickness of the recrystallized layer ($h_1$) rises. The thickness of the sintered layer ($h_2$) also increases up to a certain value of P at a relatively small traverse speed of the laser beam. However, at P > 70 W, $h_2$ begins to decrease (**Fig. 5**). It may be assumed that, at v = const, a fixed thickness of specimens, and, due to high heat conductivity of corundum [12], in the lower layers (in the sintering zone) the growth of grains ($Al_2O_3$ crystallites) occurs. As a result, the size of the sintering zone decreases. With increase in the traverse speed of the laser beam ($v$), $h_1$ and $h_2$ decrease because the heating time decreases (**Fig. 6**).

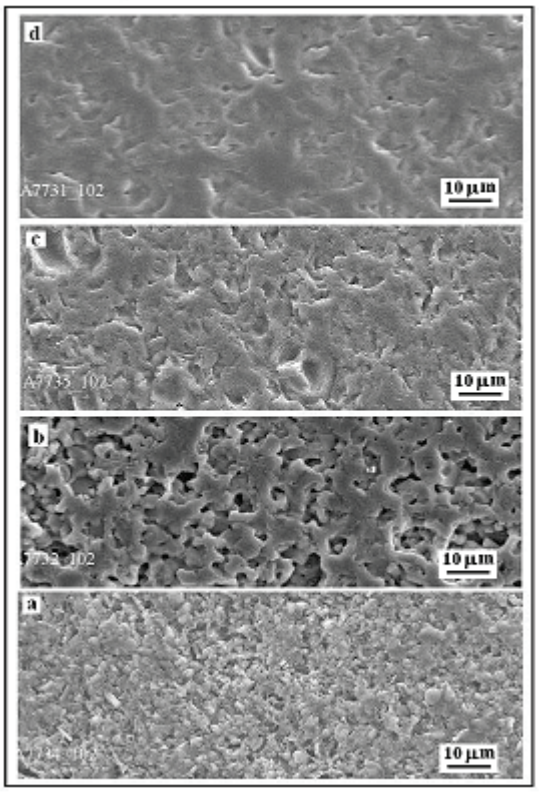


**Fig. 4.** Micrographs of channels formed in one-pass treatment at P = 70 W and v = 0.075 mm/s: (a)–(d) correspond to the direction of photographing from the bottom of the channel to its surface.

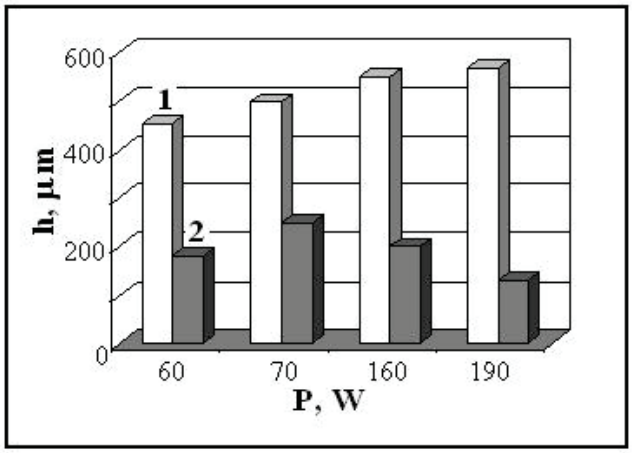


**Fig. 5.** Changes in the maximal thicknesses of the recrystallized layer (1) and sintered layer (2) depending on the power of the laser beam in one-pass laser treatment at v = 0.15 mm/s.

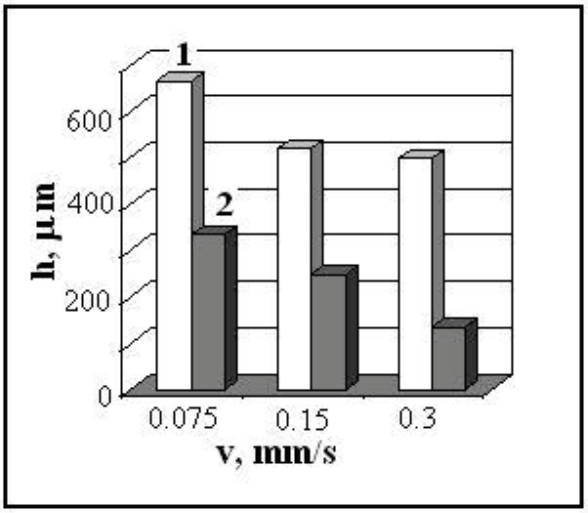


**Fig. 6.** Changes in the maximal thicknesses of the recrystallized layer (1) and sintered layer (2) depending on the traverse speed of the laser beam in one-pass laser treatment at P = 70 W.

As the layers build up, the thickness of the new-formed product (ruby) gradually increases (**Fig. 7** and **8**). In a section of the channel, boundaries of layers are seen, especially at an increased *v* (see **Fig.7 b**). This means that, in the chosen mode of treatment, not the whole volume of the backfill is melted and recrystallized. Most pores and cracks are present between the layers. From comparison of **Fig. 7 a** and **b** it is seen that the size and the number of pores increase as the traverse speed of the laser beam rises. These data show that to obtain a low-porosity track material, it is necessary to reduce substantially the traverse speed of the laser beam. As a result, a new-formed liquid phase can fill cavities, pores, and cracks of the underlying layer. Note that, as a result of the dissociation and ablation of $Al_2O_3$ [9], the largest number of cavities and channels form in the surface layers of tracks (see **Fig.7**, layers 4).

As in a case of the one-layer tracks, with decrease in *v* at a rather low power (P ~ 60–70 W), the thicknesses of the layers $h_1$ and $h_2$ increase (**Fig. 8**).

At a low traverse speed of the laser beam, a multilayered building-up of ruby (layer $h_1$) is accompanied by a decrease in the thickness of the sintered layer ($h_2$) (see **Fig. 9**). It is likely that cause of this effect is the high thermal conductivity of corundum.

The view of chips of multi-pass tracks indicates that ruby crystallites are textured in the direction to the surface of the (**Fig. 10**). Fracture predominantly occurs along grain boundaries.

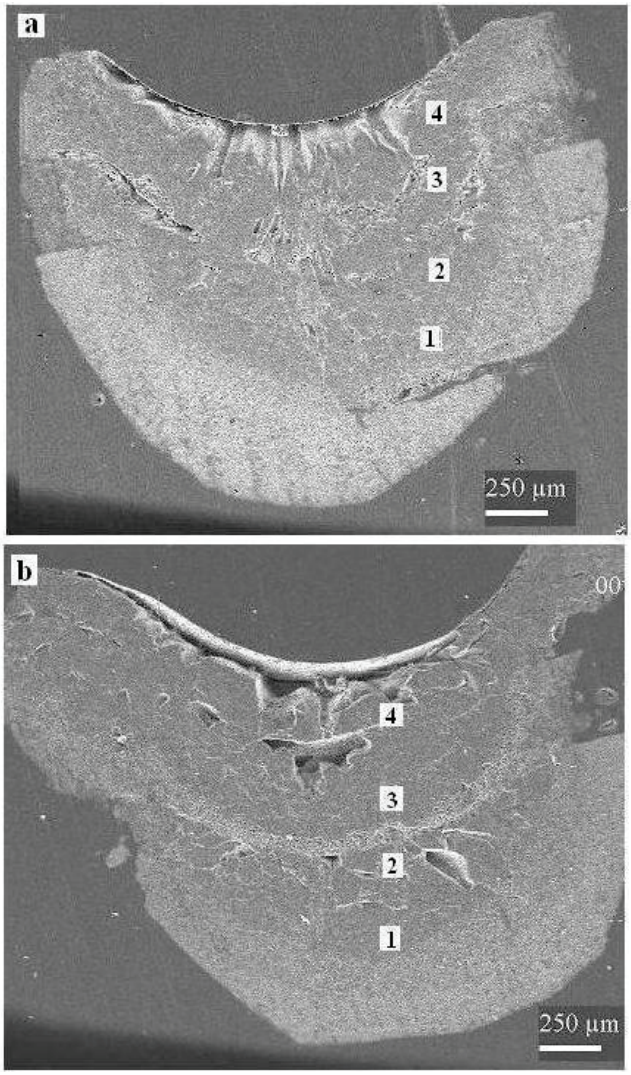


**Fig**. **7**. Micrographs of channels formed in four-run treatment. P = 70 W. (a) v = 0.075 mm/s; (b) v = 0.15 mm/s. 1–4 correspond to the numbers of layers.

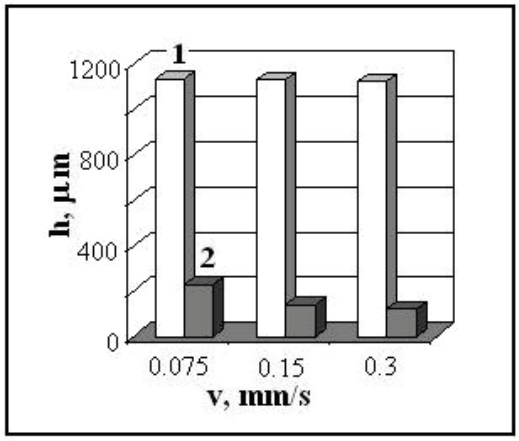


**Fig**. **8**. Changes in the maximal thicknesses of the recrystallized layer (1) and sintered layer (2) depending on traverse speed of the laser beam in four-run treatment at P = 70 W.

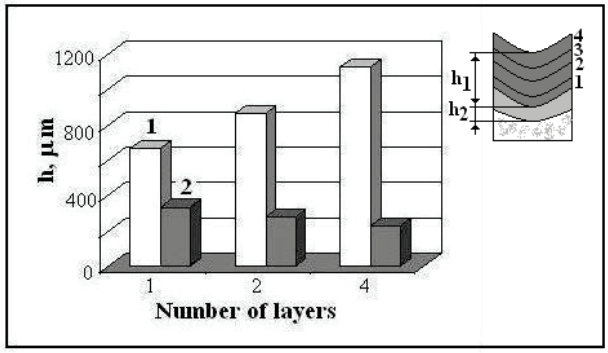


**Fig**. **9**. Changes in the maximal thicknesses of the recrystallized layer (1) and sintered layer (2) depending on the number of backfills at P = 70 W and v = 0.075 mm/s

3.3. Electron Microscopy Data Obtained under Irradiation of Isostatically Pressed Pellets

During one-pass laser treatment of dense pellets, concave tracks also forms on their surfaces. However, in this case, the depth of tracks is much smaller than that in the case of loose specimens. The thickness ($h_1$) of the formed ruby layer is ~0.3 mm even under high-power irradiation (160–190 W). The thickness of the sintering zone is comparable or slightly larger than the thickness of the recrystallization zone (**Fig. 11 a**). On a chip of a track (**Fig. 11 b**), we can see that a sintering zone transforms into a recrystallization zone and that ruby crystallites increase in size as the distance to the surface of the track decreases. On the surface of the track, cracks, boundaries of crystallites, and striation, which appears due to the ablation of the track material, are present (**Fig. 11 c**).

As is seen from **Fig. 12**, the growth of crystallites occurs from the lower layers of pellets to the surface. Crystallites are initially directed perpendicularly to the surface of the track. However, as the distance to the surface decreases, crystallites begin to deviate from vertical to horizontal direction. They take the bent shape and an identical orientation, i.e., texturing that is set by the traverse of the laser beam occurs.

In the case of quadruple building-up of layers on the surface of a track, along with defects, characteristic of one-pass treatment, overlaps of the upper layer on underlying layers (**Fig. 13 a**) are observed. On a chip of track (**Fig. 13 b**), boundaries are seen. In the contact zone of layers, the disturbance of growth of crystallites in the lower layer is noted. A new layer of ruby crystallites grows from a disordered layer. It might be assumed that in order that the boundary between the layers disappears, it is necessary to reduce the traverse speed of the laser beam and thereby increase the volume of the melted material, which captures a part of the lower layer. As in the case of one-pass treatment, growth of crystallites occurs from the lower layers of pellets to the surface. Each of the formed layers shows indications of "variable texturing", namely, vertical orientation of crystallites → horizontal orientation of crystallites (see **Fig. 12, 13 b, c**).

## 4. Discussion

The performed investigations have shown that the laser treatment of the $A1_2O_3$–$Cr_2O_3$ compacted pellets results in the formation of ruby tracks, which consist of crystallites, on their surfaces. The thickness of the tracks depends on the irradiation conditions. Under a track, a sintered layer of corundum grains is located.

The crystallite size increases as the distance to the surface decreases. Thus, the standard picture of free crystallization from melt when the lower layers cool faster than upper layers is observed [13]. The vertical texturing of crystallites is determined by the given gradient of temperatures. With increase in the irradiation power and decrease in the traverse speed of the laser beam, the efficiency of selective heating–melting of $A1_2O_3$ and the depth to which it is realized increase.

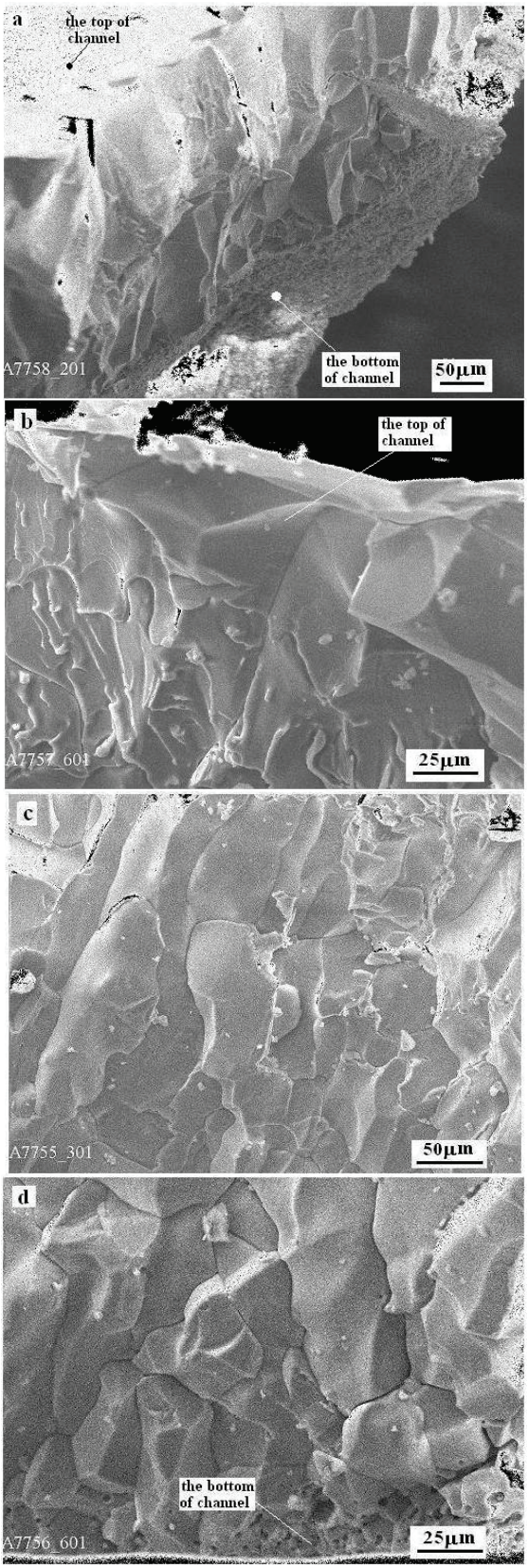


**Fig**. **10**. Micrographs of chips of a channel formed in four-pass treatment at P = 70 W and v = 0.075 mm/s.

In turn, the beam which moves discretely in a set direction initiates the movement of a part of the new-formed melt in the opposite direction (the effect of propagation of waves generated by a stone fallen into water). As a result, a moving new portion of the melt under conditions of fast cooling leads to a change in the direction of texturing of crystallites in a surface layer (**Fig. 10 b**) and forms arcs on the surface of the track.

The EPR data indicate the formation of polycrystalline ruby, i.e., along with the processes of melting and recrystallization of $A1_2O_3$, the implantation of $Cr^{3+}$ ions into the corundum lattice occurs. In this case, we can state that selective laser synthesis of ruby polycrystalline tracks takes place. The authors studied this process more thoroughly in [14].

The layer by layer selective laser sintering has revealed a number of difficulties in the preparation of a fairly homogeneous material of the channel. Even at minimal values of P and *v* used in the present work, pores and cracks are present between layers. Hence it follows that these two parameters of laser treatment should be reduced substantially and matched with one another. Thus, it will be possible to lower the temperature on a surface of a moving specimen, to melt corundum to a large depth, and reduce the intensity of ablation processes.

Results of the laser treatment of dense specimens showed that compacting pressure is an important parameter. Tracks formed by one-pass laser treatment on the surfaces of these pellets are more homogeneous. This is connected with the fact that, already in the stage of a high-pressure isostatic compaction, the conditions of shrinkage (which, in essence, are close to conditions of shrinkage in sintering) are realized [15]. As a result, the laser heating–melting process does not cause the formation of deep cavities (voids) in the primary track, which was observed in [9]. This is why the melt of the next poured layer is expended on the growth of crystallites rather than on the healing of cavities (voids) of the underlying ruby layer.

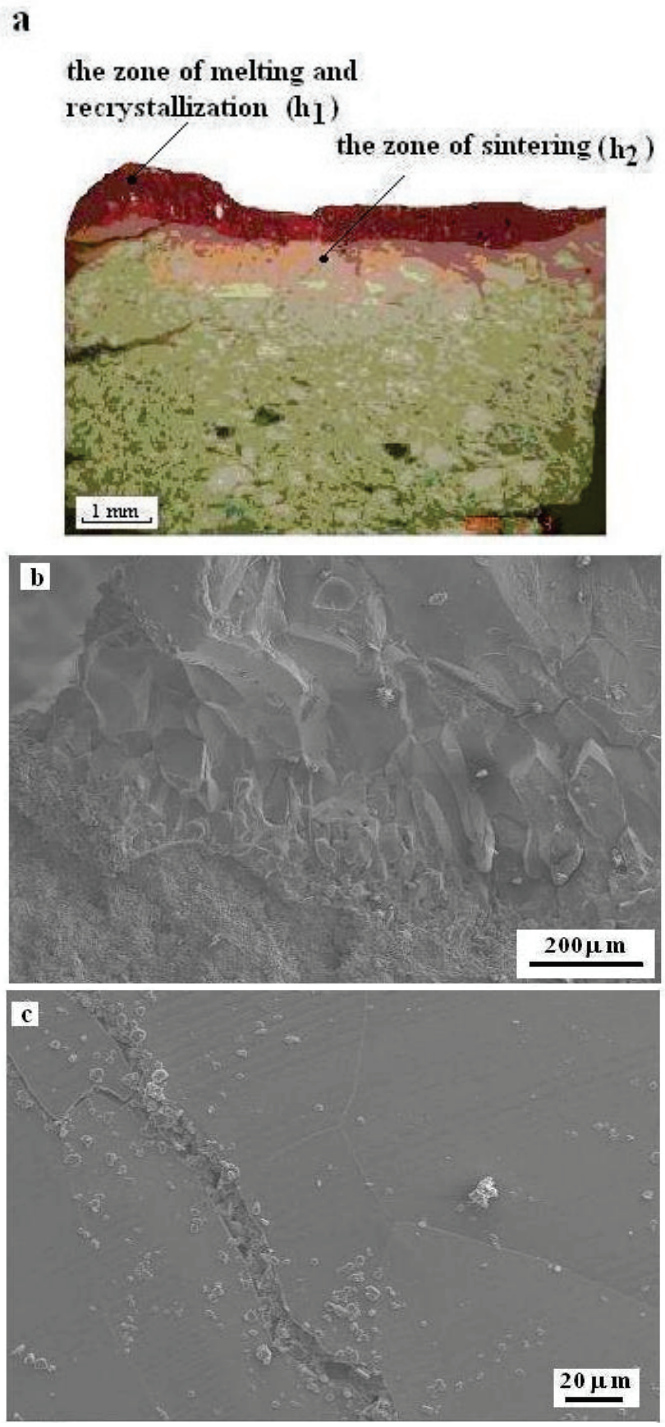


**Fig. 11**. Micrographs of a cross-section of a pellet (a), a chip of a formed channel (b), and the surface of the track (c) after one-pass treatment at P = 160 W and v = 1.25 mm/s.

The interesting feature of the formation of tracks on the surface of dense pellets is that the track material is divided more clearly into regions of volume and surface texturing of the track material (see **Fig. 12**, **I** and **V**). The growth of crystallites in the direction to the surface sets a volume texturing. The driving force of vertical texturing is a temperature gradient, namely, an increase in temperature in the direction to the surface. However, in the surface layer, a new portion of the melt with a higher temperature, which moves in the horizontal direction (and cooled) earlier formed vertically directed crystallites (the effect of a stone fallen into water») creates conditions of horizontal texturing of crystallites. On the one hand, this results in the deviation from a vertical direction of crystallites of an underlying layer (they bend taking the shape of comma), and on the other hand, to the formation of arcs on the surface of the track. The authors assume that the given effect is also connected with a specific temperature gradient, but in the horizontal direction, namely, a decrease in temperature from the point of incidence of the beam in the direction opposite to its to the direction of its traverse. The fairly good heat conductivity of corundum leads to the warming up of the top part of vertical crystallites, which take on plasticity and are bent. A generalized scheme of traverse of a laser beam over a surface of a specimen and growth of crystallites in a track is shown in **Fig. 14 a**, **c**. In **Fig. 14,** the characters of changes in the temperatures on the surface of the specimen (b) and in its volume (d) as a result of laser heating are also shown.

The more clear-cut change of a direction of texturing in more dense specimens, is evidently connected with a certain increase in the thermal conductivity in comparison with those in high porous channels formed under irradiation of loose compacts. Moreover, the temperature gradients in porous pellets may be differ from those in dense pellets, which must effect the cooling–recrystallization conditions of a surface.

The performed investigations have shown that using SLS of the $Al_2O_3$–$Cr_2O_3$ mixture it is possible to synthesize ruby and to form ruby tracks. It is assumed that the optimization of the SLS of ruby will make it possible to extend the field of application of this material in different branches of engineering.

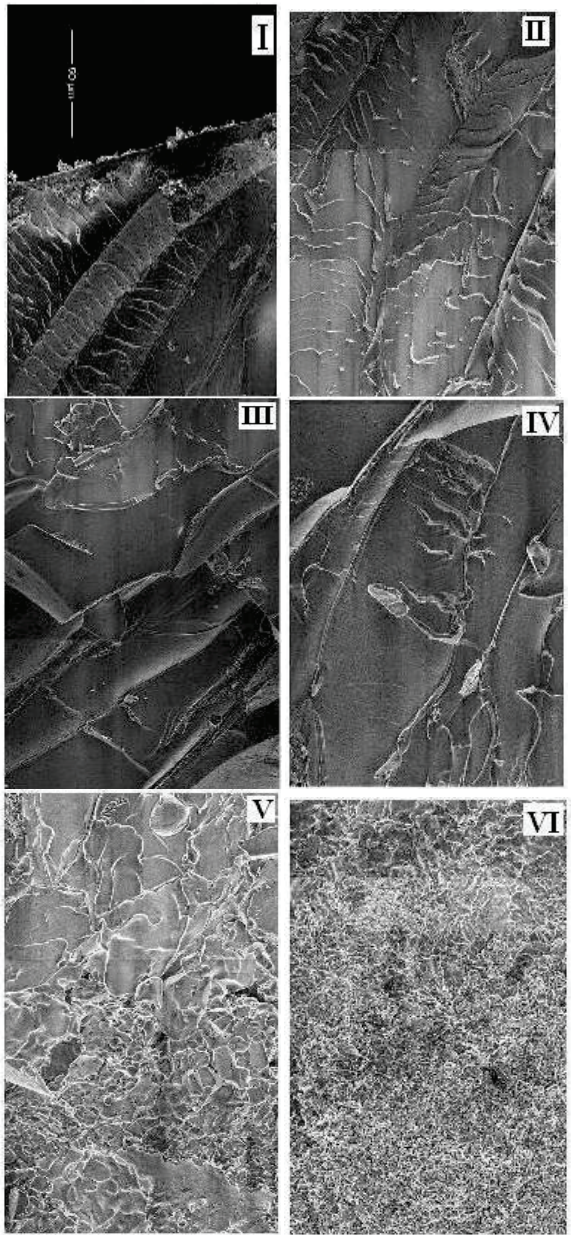


**Fig. 12.** Micrographs of the longitudinal section of channel. I-VI corresponds from the bottom to the surface of channel. The one-run treatment, P = 160 W, v = 1.25 mm/s.

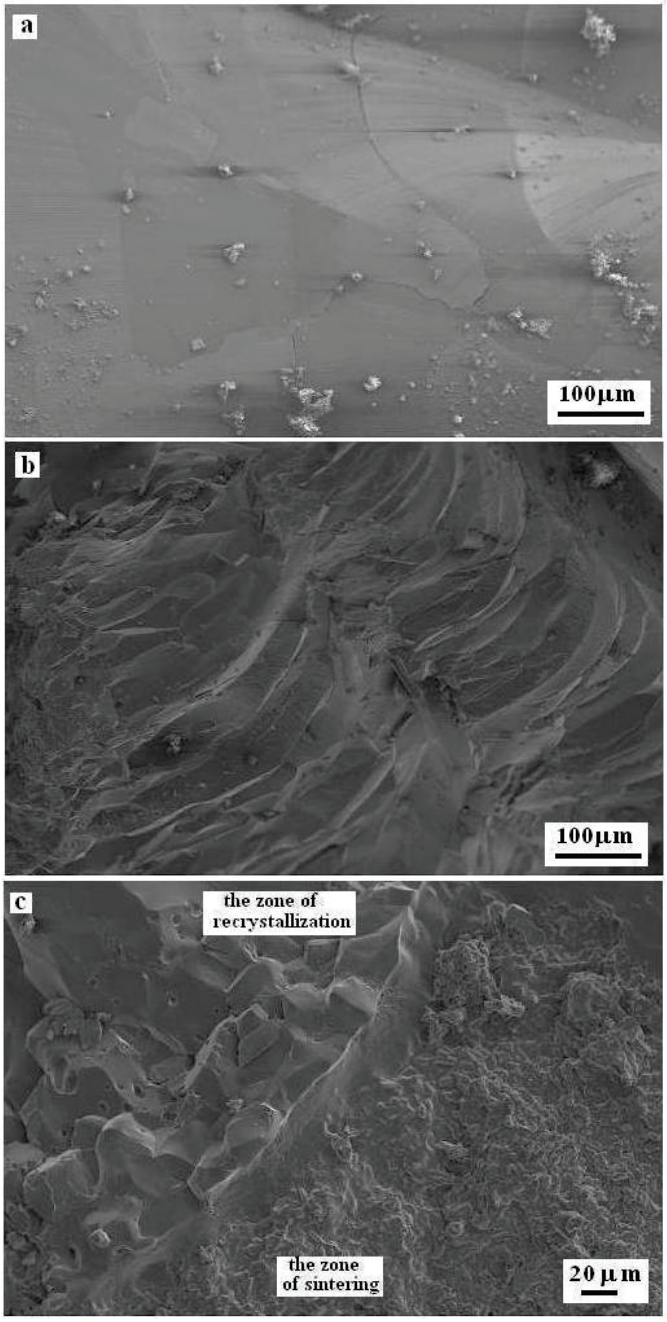


**Fig. 13**. Micrographs of the surface of a track (a), a chip of the formed track (b), and the bottom part of the track (c) after four-run treatment at P = 160 W and v = 1.25 mm/s.

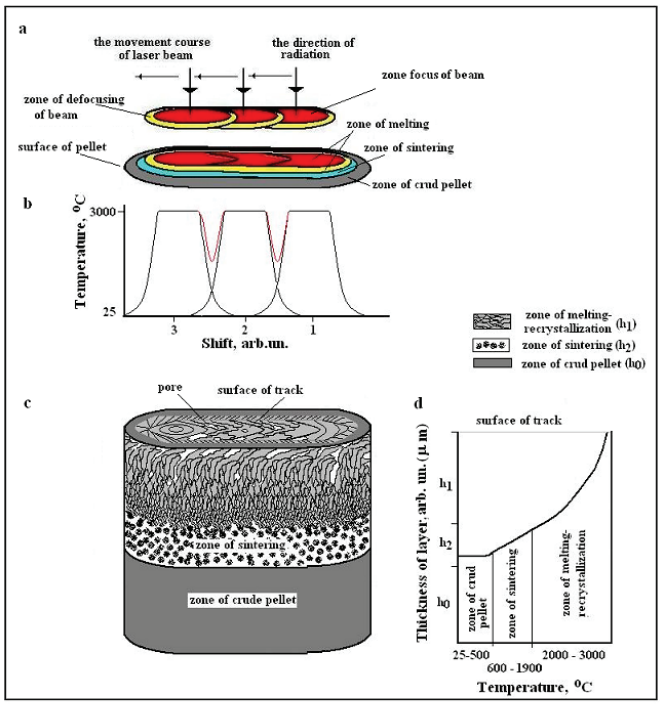


**Fig. 14.** General scheme of traverse of the laser beam (a), change in the temperature on the surface of a pellet (b), growth of crystallites in the irradiation zone (c), and variation in temperature in the volume of the pellet (d).

## 5. Conclusions

1. It has been established that layer-by-layer SLS can be used to obtain ruby tracks on the surface of pellets compacted from $Al_2O_3$ + $Cr_2O_3$ powder mixtures. This means that selective laser synthesis is realized.
2. The body of a track has a complex structure. A track proper consists of ruby crystallites. A layer of sintered ruby grains forms under the track.
3. The formation of a homogeneous low-porosity polycrystalline ruby track during layer-by-layer selective laser synthesis depends on the irradiation conditions (the irradiation power and transverse speed of the laser beam) and density of pellets.
4. In a ruby track, two types of texturing are realized. Vertical texturing of crystallites is typical of the volume layers, horizontal texturing is characteristic of the surface layer, and, in the transition region of track, the gradual deviation of crystallites from the vertical to the horizontal direction is observed.

**Acknowledgement**
The authors wish to thank CONACYT for financial support (Project 48361).
E. A. Juarez-Arellano thanks CONACyT for the fellowship provided.

**References**

1. E. Dorre and H. Hubner, Alumina Processing, Properties, and Application, (Springer-Verlag, New York, 1984).
2. Z. H. Liu, J. J. Nolte, J. I. Packard, G. Hilmas, F. Dogan, M. C. Leu, Proceedings of the 35th International MATADOR Conference, Springer, London, (2007) pp. 351.
3. P. K. Subramanian, H. L. Marcus, Materials and Manufacturing Processes., (1995) p.10.
4. I. V. Shishkovskii, Laser Synthesis of Functional Mesostructures and Bulk Articles [in Russian], "(Fizmatlit", Moscow, 2008).
5. Z. Xu, J. Zhang, H.Zheng, C. Cai, Y. Huang, J. Mater. Sci. Technol., 21, (2005) 866.
6. I. Shishkovsky, I. Yadroitsev, Ph. Bertrand, I. Smurov, Applied Surface Science., 254, (2007) 966.
7. P. K. Subramanian, G. Zong, N. Vail, J W. Barlow, and H. L. Marcus, Solid Freeform Fabrication Proceedings, (1993) p.350.
8. Murotani Hirishi, Mitsuda Takahiko, Wakaki Moriaki, Kondo Yoshinori, Proceedings of the School of Engineering of Tokai University, (1999) p. 95.
9. M. Ristich , M. Vlasova, A. Ragulya, V. Stetsenko, M. Kakazey, P. A. Marquez Aguilar, I. Timofeeva, T. Tomila, E. A. Juarez Arellano, Report on "International Conference Sintering", (2009).
10. A. A. Manenkov, and A.M. Prokhorov, Soviet Phys. – JETP, 1, (1955) 611.
11. A. Knappwost, and W. Gunsser, Phys. Chem. N.F., 21, (1959) 305.
12. Handbook of physical-chemical properties of oxides. (Ed. G.V. Samsonov, Metallurgia, Moscow, 1978).
13. M. V. Klassen-Neklyudova, Ruby and Sapphire. (Nauka. Moscow, 1974). 236.
14. M. Kakazey, M. Vlasova, P. A. Marquez Aguilar, A. Bykov, V. Stetsenko, A. Ragulya., Int. J. Applied Ceramic Technology, 6, (2009). 335.
15. R. M. German, Sintering Theory and Practice, (Wiley-VCH 1996), 568.

(Received: November 17, 2010, Accepted: March 15, 2011)